Theoretical and Experimental Studies of Carbon Nanotube Electromechanical Coupling

A. Z. Hartman,[1] M. Jouzi,[1] R. L. Barnett,[2] and J. M. Xu[1]

[1]*Division of Engineering and Department of Physics, Brown University, Box D, Providence, Rhode Island 02912, USA*

[2]*Physics Department and Division of Engineering and Applied Science, Harvard University, 02138 Cambridge, Massachusetts, USA*

(Received 24 October 2003; published 11 June 2004)

We present an investigation into electromechanical coupling in carbon nanotubes by focusing on phonon frequency shifts as a result of charge injection. A nearest-neighbor, tight-binding theoretical model is accompanied by a computational explication carried out using the Vienna *ab initio* simulation package density functional theory code. Raman spectroscopic measurements of the electromechanic couplings under varied but controlled charge injection conditions are also carried out, and the close agreement between the model results and the measured Raman peak shifts suggests that geometrical changes of charged carbon nanotubes previously observed or speculated in different experiments can indeed originate from the simple quantum effects described herein.

DOI: 10.1103/PhysRevLett.92.236804 PACS numbers: 73.22.–f, 63.22.+m, 71.15.Mb, 71.15.Pd

Introduction.—Carbon nanotubes (CNTs) are currently being pursued as a unique new class of materials possessing remarkable electrical and mechanical properties and offering great promises for applications [1]. Consequently, a large body of literature reporting on the electronic and mechanical properties of CNTs has gradually emerged, along with theoretical and experimental studies pertaining to the their remarkable and diverse electrical properties. It is therefore natural to pursue an investigation into the coupling between the electrical and mechanical effects in CNTs. This coupling has been investigated recently in the literature [2,3], which has proposed, among other ideas, a Hamiltonian with a term that demonstrates a tight coupling between the electronic and atomistic degrees of freedom.

The several models that have been presented recently represent the first attempts at establishing a basic understanding of the electromechanical coupling in single-walled carbon nanotubes (SWNTs) [1,2]. Given that such studies are intensively numerical in nature, with *ab initio* simulations taking the principal foreground, the findings are heavily dependent on each model's own sphere of assumptions, much of which are specific to a particular idealized CNT. It is thus desirable to approach the problem both with a theoretical method that is as context independent as possible, in an attempt to understand the fundamental physics responsible for this electromechanical coupling, and then to compare the results with computational and direct experimental observation.

Possible reasons for the lack of direct experimental findings are the many difficulties associated with measuring small perturbations on already small objects. In the case of many nanotubes used to aggregate the signal, one suffers from the difficulties in interpreting the results from a large number of nanotubes of different diameters, lengths, bending, and entanglement.

In this Letter we take a comprehensive approach, combining theory with experiment, to the problem. First we formulate the problem in the context of a simple theoretical model, which pays little attention to the specific atomistic details, focusing instead on the fundamentals of the coupling between adjacent atoms. As is often done for simplicity, we focus only on the orbitals of the π electrons, although in a more detailed context the σ electrons and the effects of σ-π hybridizations may play a role [3–5]. We next examine the details of the electromechanic couplings in specific model nanotubes in the framework of the density functional theory (DFT) of Hohnberg and Kohn [6,7], as done previously [1,2]. These simulations have tended to yield results that agree qualitatively with one another in certain contexts, but often disagree in details [1,2]. In the following, we compare computational with theoretical results and present an experimental validation for these ideas by use of a devised Raman spectroscopic approach, through which we directly measure the mechanic responses to excess electron injection (or extraction).

Theoretical model.—We consider the geometry of the nearest-neighbor tight-binding (NN-TB) model of a graphite sheet, in the spirit of [1] and shown in the inset of Fig. 1, in which to induce a slight deviation in the total energy and derive from it an expression for the resultant spectrum of lattice-coupled phonon modes in the regime of slight excess charging.

Considering the geometry shown in the inset of Fig. 1 we write out the NN-TB expression for the energy spectrum for a deformed lattice with hopping parameters t_A and t_B ε_k as

$$\varepsilon_{\mathbf{k}} = \varepsilon_{2p} \pm [t_A^2 + 2t_A t_B[\cos(\mathbf{k}\cdot\mathbf{a}_1) + \cos(\mathbf{k}\cdot\mathbf{a}_2)] + 2t_B^2\{1 + \cos[\mathbf{k}\cdot(\mathbf{a}_1 - \mathbf{a}_2)]\}]^{1/2}, \quad (1)$$

where ε_{2p} is the closed shell energy of the p_z orbital, assumed to be near the Fermi energy ε_F for this particular case. We are specifically interested in slight deformations in k space, which we examine by expanding around

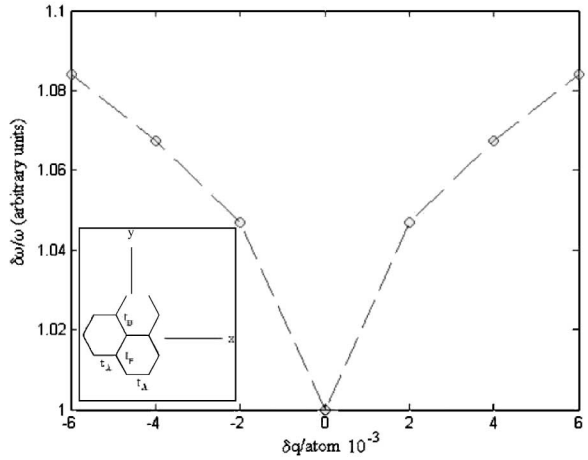

FIG. 1. Theoretical prediction for the expected shift in frequency due to electron-phonon coupling, due to lattice distortion, in arbitrary units. There is an abrupt dropoff in frequency shift at zero charging. (Inset: nearest-neighbor tight-binding geometry for graphite sheet, with overlap integrals.)

the point $\mathbf{K} = \frac{2\mathbf{b}_1+\mathbf{b}_2}{3}$, where $\mathbf{b}_1$ and $\mathbf{b}_2$ are the reciprocal lattice vectors, to obtain

$$\varepsilon_{\mathbf{k}} = \varepsilon_{2p} \pm [(t_A^2 + t_B^2) - (t_B^2 - t_A t_B)k_y\sqrt{3} + \tfrac{3}{4}(t_A t_B)k_x^2 + \tfrac{1}{4}(t_A t_B + 2t_B^2)k_y^2]^{1/2}. \quad (2)$$

We expect from the geometry of the p_z orbitals that the overlap integrals will have functional dependences such that $t_i = t_i(\Delta)$, where Δ is the the magnitude of the distortion. With this in mind we can now expand the two overlap integrals in Δ, and keeping terms to leading quadratic order we find that

$$t_A = t(1 + \alpha\Delta + \beta\Delta^2), \quad (3)$$

$$t_B = t\left(1 - \alpha\frac{\Delta}{2} + \left\{\frac{\beta}{4} + 3\sqrt{3}\frac{\alpha}{4}\right\}\Delta^2\right) \quad (4)$$

for constants α and β. By using these values for the hopping integrals, we can obtain the charge-dependent spring constant which can be written as

$$\kappa(q) = t(q)\sum_{\mathbf{k}\in\mathrm{occ}} \frac{\partial^2 \varepsilon_{\mathbf{k},\Delta}}{\partial\Delta^2|_{\Delta=0}}, \quad (5)$$

where the sum is carried out over occupied states which, in turn, depend on the net charge q. The above sum can be carried out along the quantization lines for the specific nanotube under consideration to yield

$$\omega(q) \sim \kappa(q)^{1/2} \sim \sqrt{(A + B|q|)}, \quad (6)$$

where A and B are constants depending on the nanotube under consideration.

Hence we have a direct relationship between the phonon modes we expect to see excited in the lattice due to a slight distortion in the energy by addition of a small amount of charge q, shown explicitly in Fig. 1. Qualitatively the oscillations are slightly asymmetric about the sharp point when $q = 0$ (equivalently, zero gating), and demonstrating a general behavior that agrees well with the results of DFT-based simulations, and direct experimental observations, given in the next two sections, respectively.

Density functional theory computations.—DFT simulations were carried out using the Vienna *ab initio* simulation package (VASP) code [8]. Our computations use a $9 \times 9 \times 9$ grid centered at the Γ point, and an ultrasoft carbon psuedopotential with a Wigner-Seitz radius of $r = 1.640$ Å, in a frozen-phonon, non-spin-polarized calculation, in which the electronic structure of the CNTs were allowed to relax. We used ultrasoft projector augmented wave potentials for carbon.

We consider first the special cases of $(N, 0)$ and (N, N) SWNTs, demonstrating the phonon frequency as it depends on the injected charge, choosing our N such that $N > 5$, since the case of $(5, 0)$ tubes has been noted to mark a particularly interesting case, which the present theoretical model is not suited to handle [9].

Figure 2 shows the computational results, carried out for the specific cases of $(6, 6)$ and $(7, 0)$ SWNTs where each data point represents a fully self-consistent calculation for the specified charge density, containing 24 and 28 carbon atoms per unit cell, respectively. It is clear that qualitatively the behavior exhibited in both the $(N, 0)$ and (N, N) cases exhibits a similarity to the results for the simple theoretical model in the previous section, at least qualitatively.

Experimental observation.—We use Raman spectroscopy of the uniform multiwalled CNTs to verify what we discussed in the previous sections. Usual basic Raman modes in CNTs are RBMs (radial breathing modes),

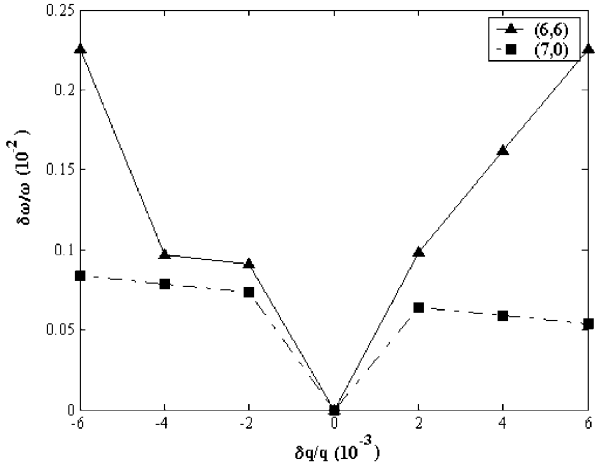

FIG. 2. VASP simulation for (N, N)- and $(N, 0)$-type carbon nanotubes. Both traces exhibit an asymmetry about the negative-positive charging regimes, as well as abrupt behavior at zero gating.

which occur between 100–300 cm^{-1}, the G band (tangential) at 1600 cm^{-1}, the D band (disorder induced) at 1300–1400 cm^{-1}, and the G' band at 2600–2800 cm^{-1} [10]. Other peaks in the spectrum arise from the anti-Stokes processes. In a defect-free graphite sheet the Raman spectra contain all these peaks except for the D band, which originates from double resonant Raman scattering from defects [10–13]. In this process the excited electron will experience double scattering from a phonon and a defect, and, therefore, by increasing the number of sp^3 bonds in a graphite sheet the intensity of the D band will increase. The RBMs are responsible for out-of-plane atomic vibrations, while the in-plane vibrations produce the G band [13]. The origin of the G' band is double scattering, like the D band, but here both scatterings are due to phonons, so the peak is present regardless of any defect in the system [11].

In [14] the different active phonon modes (with different symmetries) in a SWNT have been discussed, as well as shown by simulation that the D band in $(N, 0)$ or (N, N) SWNTs consists of five different phonon modes, while for the G band this number is three, giving a sharper peak, as we have seen experimentally. All the out-of-plane vibrations fall in the low frequency portion of the spectrum, whereas the G- and D-band modes are all in plane. If there is any change in resonant frequency due to the C-C bond change, it will show up more visibly in the corresponding G- and D-band spectra.

In addition to the fact that the G band has a sharper peak and in which it is therefore easier to detect shifts than in the D band, there are several reasons for us to consider the G-band peak for our investigation. The D band is sensitive to the diameter distribution of, and to, the stacking and bundling coupling between the tubes in the sample [10], while the G band is much less so, especially for large diameters [14]. Also, due to the double resonance origin of the D band, its position will shift with respect to the excitation energy, while the G-band positions are not expected to change with excitation energy, as previously reported [11–13].

For the sake of interpreting experimental measurements, it is highly desirable to have a high degree of uniformity in the CNTs, which is generally absent in samples obtained via conventional processes based on arc discharging, laser ablation, or chemical vapor deposition. The resultant CNTs in those methods differ widely in their diameter and length and therefore also in their physical properties. Moreover, they often come in the form of entangled bundles mixed with other particles and residual materials. Fortunately, a relatively new template-based fabrication approach demonstrated by our group offers a promising solution to the problem [8].

The growth process yields multiwalled carbon nanotubes (MWNTs), which are uniform in diameter, length, orientation, and spacing. Although for modeling purposes SWNTs are ideal and more manageable in computation, in experiment they are much more difficult to deal with because of the large dispersion in diameter, length, and chirality inevitable in even the smallest sample that would allow for a clear reading of the Raman spectral shift. Indeed, multiple trials on SWNT samples failed to show any discernible shifts with charging, most likely due to the smearing of the peak shifts due to the large structural dispersions and the stacking of the nanotubes, which give rise to effects mimicking that of defects within individual tubes. By contrast the great uniformity of the MWNT samples chosen for this study proved indispensable to the experiments reported here. And since the principal effects of the electromechanical couplings studied in this work arise primarily from the local bond deformation and hybridization in response to the excessive electronic charge (long-range coherence effects are ignored theoretically), this makes the comparison of our results with our theoretical predictions a valid one.

We dispersed uniform CNTs on a Si-SiO_2 wafer (SiO_2 thickness 250 nm) and then evaporated a thin, nearly transparent gold layer, over half of the mat of the CNTs ($\sim$10 mm^2), as illustrated in Fig. 3(a). It can be seen that although our CNTs are straight, and uniform in length and diameter, they are also stacked, which induces effects equivalent to an increase in the defect concentration distribution and hence broadening of the D band. We measured the capacitance of this parallel plate configuration to be 1.2 nF. By then applying different voltages across the sample we controllably varied the amount of static charge present on the sample, under the imposed constraint of near-zero leakage current. As a rough estimation, using the measured geometric parameters in the experiment, we can estimate an excess of charge of

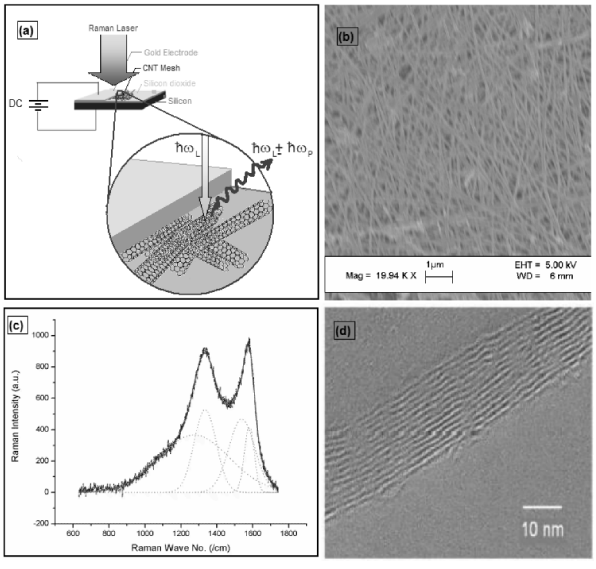

FIG. 3. (a) Schematic view of the experiment setup. (b) A view of carbon nanotube mesh on the wafer. (c) Raman spectrum of carbon nanotubes and Gaussian fits of Raman peaks (dashed lines). (d) High resolution TEM image of our multiwall carbon nanotubes.

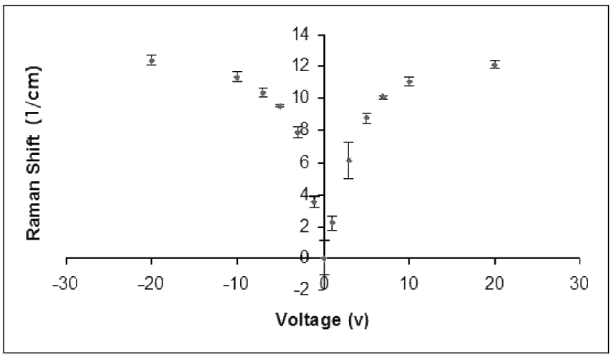

FIG. 4. The measured shift of the *G*-band peak with applied voltage (charge) of both polarities.

10^{-16} C on each CNT with respect to a 1 V potential across the sample.

In setting up the Raman measurements, approximately 5 mW laser power was focused on a 2 μm sample spot. The laser induced heating, as measured through the Raman Stokes and anti-Stokes peaks, and evidenced through the sample transparency change observable through microscopic observation, can raise the local spot temperature over 1000 °C and help anneal the CNTs. From independent experiments conducted by our group, and reported in the literature, it is known that laser annealing of chemical vapor deposition synthesized MWNTs can substantially improve their crystallinity. However, during the actual Raman measurements, we used the lowest laser power possible to minimize any heating in order to avoid a possible heating induced change in phonon frequency [15]. We have furthermore eliminated the possibility of misattributing the cause of the shift by fitting several Raman spectral peaks to Gaussian curves, with the same statistical parameters, so that the relative shift due to charging is clearly discernible, as seen in Fig. 3(c).

Figure 4 shows the measured shift of the *G*-band peak with applied voltage of both polarities. Considering this observed result we can make some comparisons with the results of the previous sections, which we believe are possible to draw for the following reasons. First, we believe we can eliminate the possibility of the phonon shift being due to the effects of laser heating since we expect that this will shift the peak in the opposite direction. Second, we believe that the results obtained for the sample composed of MWNTs is suitable for comparison to the theoretical and computational results since their relatively large circumferences make them more suitable for this measurement due to the fact that their *G*-band peaks are less likely to change due to variations of the diameter, in which case the shift can be more reliably attributed to the lattice change. Quantitatively we see that in the case of the computational results the phonon modes in Fig. 1 span a total shifted range of $|\frac{\delta\omega}{\omega}| \sim 8\%$, whereas the computations in Fig. 2 give $|\frac{\delta\omega}{\omega}| \sim 0.23\%$ for the $(6, 6)$ nanotube and $|\frac{\delta\omega}{\omega}| \sim 0.8\%$ for $(7, 0)$, an order of magnitude difference. However, the restraints on the constants A and B in the analytic model permit some arbitrary modulation [anything to within $O(\Delta^2)$] in which case it can be tuned into closer agreement, which we believe to be acceptable considering its approximations of a closed $2p$ shell, no interorbital hybridizations, etc. In addition, the fact that the three different approaches yield qualitatively similar results provides a guidepost for certain behaviors which MWNTs and SWNTs are expected to share in common and may indeed be an indicator that these behaviors are dominated by local short-range electromechanic couplings rather than a long-range effect.

This work was made possible by support from the DARPA NMASP program and by valuable assistance received from Dr. M. Tzolov.

[1] Y. N. Garstein *et al.*, Phys. Rev. Lett. **89**, 045503 (2002).
[2] M. Verissimo-Alvez *et al.*, Phys. Rev. B **67**, 161401(R) (2003).
[3] A. Rakitin, C. Papadopoulos, and J. M. Xu, Phys. Rev. B **61**, 5793 (2000).
[4] X. Blase *et al.*, Phys. Rev. Lett. **72**, 1878 (1994); C. Papadopoulos, A. Rakitin, and J. M. Xu, Phys. Rev. B **67**, 033411 (2003).
[5] Y. Guo and W. Guo, J. Phys. D **36**, 805 (2003).
[6] P. Hohenberg and W. Kohn, Phys. Rev. **136**, B864 (1964).
[7] W. Kohn and L. J. Sham, Phys. Rev. **140**, A1133 (1965).
[8] O. Dubay and G. Keresse, Phys. Rev. B **67**, 035401 (2003).
[9] T. Lenosky, X. Gonze, M. Teter, and V. Elser, Nature (London) **355**, 333 (1992).
[10] M. E. Dresselhaus, G. Dresselhaus, and P. C. Eklund, *Science of Fullerenes and Carbon Nanotubes* (Academic, New York, 1996).
[11] H. Kuzmany *et al.*, Phys. Rev. B **65**, 165433 (2002).
[12] C. Thomsen and S. Reich, Phys. Rev. Lett. **85**, 5214 (2000).
[13] H. Kuzmany *et al.*, Phys. Rev. Lett. **90**, 157401 (2003).
[14] R. A.-Jishi and G. Dresselhaus, Phys. Rev. B **26**, 4514 (1982).
[15] N. R. Raravikar *et al.*, Phys. Rev. B **66**, 235424 (2002).